Synthesis and characterization of chitosan/TiO$_2$ nanocomposite for the adsorption of Congo red

Umma Habiba[a], Tan Chin Joo[a], S.K.A. Shezan[b], Rasel Das[c], Bee Chin Ang[d], Amalina M. Afifi[a],*

[a]*Centre of Advanced Materials, Department of Mechanical Engineering, Faculty of Engineering, University of Malaya, Kuala Lumpur, 50603, Malaysia, email: habiba_buet@yahoo.com (U. Habiba), tanchinjoo@siswa.um.edu.my (T.C. Joo), amalina@um.edu.my (A.M. Afifi)*
[b]*School of Engineering, RMIT University, Melbourne, Australia, email: shezan.ict@gmail.com (S.K.A. Shezan)*
[c]*Global Innovation Centre (GIC), Kyushu University, Fukuoka 816-8580, Japan, email: raselgeneticist@gmail.com (R. Das)*
[d]*Centre of Advanced Materials, Department of Chemical Engineering, Faculty of Engineering, University of Malaya, Kuala Lumpur, 50603, Malaysia, email: amelynang@um.edu.my (B.C. Ang)*

Received 4 February 2018; Accepted 13 May 2019

ABSTRACT

Chitosan/TiO$_2$ nanocomposite was fabricated by a film-casting method for the adsorption of Congo red. The nanocomposite film was characterized by Fourier transform infrared spectroscopy, field-emission scanning electron microscopy, powder X-ray diffraction, thermogravimetric analysis, weight-loss test, and adsorption study. Morphological analysis revealed rough and agglomerated filler materials over the film surface. The interaction among components of the composite was proven by powder X-ray diffraction and Fourier-transform infrared spectroscopy. The weight-loss result showed excellent stability of the composite in acidic medium. The adsorption mechanism was supported by both Langmuir and Freundlich isotherm models. The adsorption capacity of the composite film was 32 mg/g.

Keywords: Adsorption; Carbohydrate; XRD; TiO$_2$

1. Introduction

Industrial effluents are causing significant environmental pollution. Organic dyes are major constituents of industrial effluents. Dye removal from water is difficult because of its inertness. In recent years, many methods have been developed for dye removal and water treatment. Some favorable methods are reverse osmosis, flocculation [1], bacterial action, adsorption [2,3], and photo catalytic degradation [4]. Among them, adsorption is simple, highly efficient, and easy. The use of adsorbents for water treatment is being extensively studied. TiO$_2$ is a key material in the degradation of organic pollutants [5]. TiO$_2$ has a high surface area and affinity to dye molecules [6] but is susceptible to agglomeration during operation, so it cannot stand be used alone for water treatment. By contrast, it can perform well with a polymer with a film-forming capability [7].

Chitosan is commonly used for chemical immobilization because of its extraordinary attributes, such as hydrophobicity, biocompatibility, biodegradability, environment friendliness, and adsorption properties. Chitosan can be used as an adsorbent to expel overwhelming metals and colors because of the proximity of amino and hydroxyl groups, which can fill in as dynamic end groups. The amino groups of chitosan can be cationized, after which they completely adsorb anions through electrostatic interaction in acidic media [3,8,9]. Nevertheless, chitosan is exceptionally sensitive to pH as it can either take a gel form or break up depending on the pH. To enhance chitosan's adsorption properties, many researchers have used cross-connecting reagents such as glyoxalin, formaldehyde, glutaraldehyde, epichlorohydrin, ethylene glycol diglycidyl ether, and iso-

*Corresponding author.

cyanides. Cross-connecting reagents balance out chitosan in corrosive arrangements such that it becomes insoluble and also improves its mechanical properties [10]. However, most of these reagents are either expensive or toxic. The major limitation of chitosan as an adsorbent is that it only transfers dye molecules from the solution to its surface, meaning that the dye content cannot be eliminated permanently. Conversely, TiO_2 nanoparticles can destroy the molecular backbone of dye molecules. It can also be regenerated for subsequent dye removal. A chitosan/TiO_2 composite can reportedly be used to remove Rhodamine B, methyl orange, methylene blue, and Pb (II) [11–14].

In the present work, chitosan/TiO_2 nanocomposite was synthesized by a film-casting method. Field-emission scanning electron microscopy (FESEM), powder X-ray diffraction (XRD), Fourier transform infrared spectroscopy (FTIR), thermogravimetric analysis (TGA) and weight-loss analysis were then conducted for the morphological and structural analyses. Finally, the adsorption capacity of the resulting composite for Congo red was evaluated.

2. Experimental

2.1. Materials

The TiO_2 nanoparticles were obtained from Sigma–Aldrich, Malaysia. Congo red and chitosan were purchased from R&M chemicals and SE Chemical Co., Ltd., Japan, respectively.

2.2. Methods

2.2.1. Chitosan hydrolysis

Chitosan solubility depends on deacetylation degree. The deacetylation degree of the supplied chitosan was 40% and it was not completely soluble in acidic medium, so deacetylation was required. First, 40 g of NaOH was stirred in 80 g of distilled water, and then 2.5 wt.% chitosan was added and stirred with the NaOH solution for 12 h at 90°C. Second, chitosan was filtered and dried for 7 h at 60°C after subsequent washing with distilled water.

2.2.2. Synthesis of chitosan/TiO_2 nanocomposite

Chitosan/TiO_2 nanocomposite was prepared by film-casting method. First, 2 wt.% chitosan was dissolved in 90% acetic acid. Second, 1 g of TiO_2 was magnetically stirred with 10 ml of chitosan solution. The solution was stored in a Petri dish to dry for 7 h at 70°C. Finally, the composite was rinsed with aqueous NaOH and oven dried at 70°C. The schematic of the chitosan/TiO_2 preparation is shown in Fig. 1.

2.2.3. Characterization

Elemental analysis of the composite was conducted by FTIR and XRD techniques. A Nicolet iS10 FTIR spectrometer (Thermo Scientific; 600 to 3000 wave numbers, resolution of 4 cm^{-1}) was used for FTIR analysis. A PAN analytical empyrean X-ray diffractometer (λ = 1.54060 Å, Cu K$_\alpha$ radiation) was used for XRD analysis. Morphological analysis
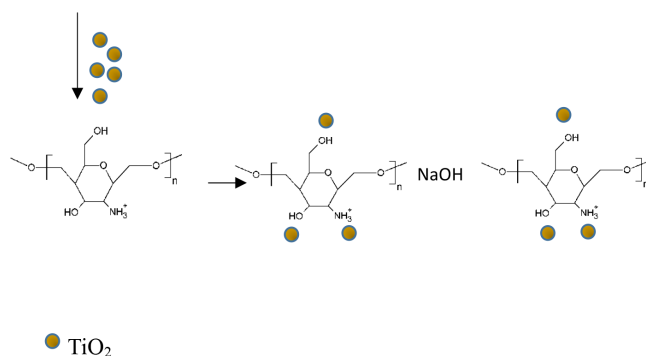
Fig. 1. Schematic of chitosan/TiO_2 preparation.

was conducted with a FESEM system (Zeiss Auriga). Thermal properties were examined with a thermogravimetric analysis (TGA) apparatus (SETARAM TGA 92) at a heating rate of 20°C/min and 30–800°C.

2.2.4. Weight-loss test

Weight-loss test was performed to determine the stability of the composite. The weight of the chitosan/TiO_2 nanocomposite was initially determined before dipping in acidic (pH 3) medium for 10 days at room temperature. After collecting the composite, it was stored at room temperature for drying. Then, the dried sample was weighed and the weight-loss percentage was calculated using the equation below:

$$Weight\ loss(\%) = \frac{W_0 - W_1}{W_0} \times 100 \qquad (1)$$

where W_0 and W_1 are the masses before and after dipping in acidic medium, respectively.

2.2.5. Adsorption test

The adsorption test of Congo red was carried out by varying the initial concentration of Congo red solution. About 50 mg of the composite was added to 10 ml of Congo red solution, and the mixture was stored at room temperature until equilibrium was obtained. The composite was then collected and subjected to ultraviolet–visible spectrophotometry (Varian CARY 50 probe) to determine the dye-solution concentration. The amount of adsorbed Congo red was calculated using the equation below:

$$q_t = \frac{(C_o - C_t)}{m}V \qquad (2)$$

where q_t (mg/g) is the amount of dye adsorbed, C_o and C_t (mg/L) are the initial and final dye concentrations, respectively, m (g) is the mass of adsorbent and V (L) is the volume of the dye solution.

3. Results and discussion

3.1. FESEM analysis

FESEM analysis was performed to analyze the composite morphology and the dispersion of TiO_2. Fig. 2 shows the
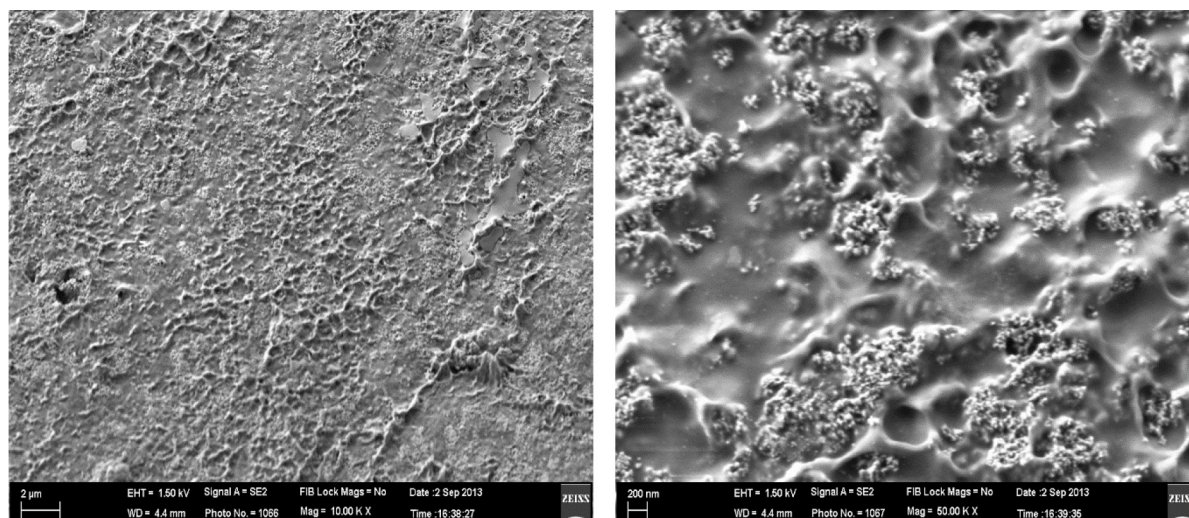
Fig. 2. FESEM image of chitosan/TiO$_2$ composite.

FESEM image of chitosan/TiO$_2$ nanocomposite. The surface was very rough and uneven. Surface roughness is an important factor for ensuring high adsorption efficiency by increasing hydrophilicity [15,16]. The filler particles, TiO$_2$, are supposed to agglomerate because of Van der Waals forces. Thus, inter facial adhesion between chitosan matrix and TiO$_2$ particles is believed to be poor [17]. Similar findings have been previously reported [18,19].

3.2. XRD analysis

The XRD spectra of chitosan, TiO$_2$, and chitosan/TiO$_2$ nanocomposite are shown in Fig. 3. The strongest peaks of TiO$_2$ were observed at 2θ = 25.27°, 27.42°, 37.78°, and 48°. According to JCPDS (Reference code: 00-002-0514), these peaks belonged to the brookite phase of TiO$_2$. The XRD peaks of pure TiO$_2$ were clearly observed in the XRD plot of the composite, indicating that TiO$_2$ crystallinity was not lost in the chitosan matrix. However, the peak intensity was altered because of the H-bonding between chitosan and TiO$_2$ [20–22]. For chitosan, strong peaks at 2θ around 9°–10° and 20° were attributed to –OH and –NH$_2$. These peaks, including minor reflection at higher 2θ values, signify that it was α-chitosan [23,24]. The crystalline peaks of chitosan almost vanished in the composite. A possible reason was the bond formation of chitosan with TiO$_2$.

3.3. FTIR analysis

Fig. 4 shows the FTIR analysis of chitosan, chitosan/AcOH, and chitosan/TiO$_2$ nanocomposite. The peak at 660 cm^{-1} was the crystalline sensitive band of chitosan [25], and it disappeared after dissolving chitosan in acetic acid. The probable reason was the hydrogen bonding of chitosan with acetic acid. Thus, in accordance with the XRD study, chitosan lost its crystallinity to some extent. The peak at 709 cm^{-1} was attributed to Ti–O–Ti [26]. The characteristic peak of the saccharide group of chitosan was at 1151 cm^{-1} [27]. The peak at 1573 cm^{-1} was for the N–H bending of chitosan [20]. This peak intensity increased and
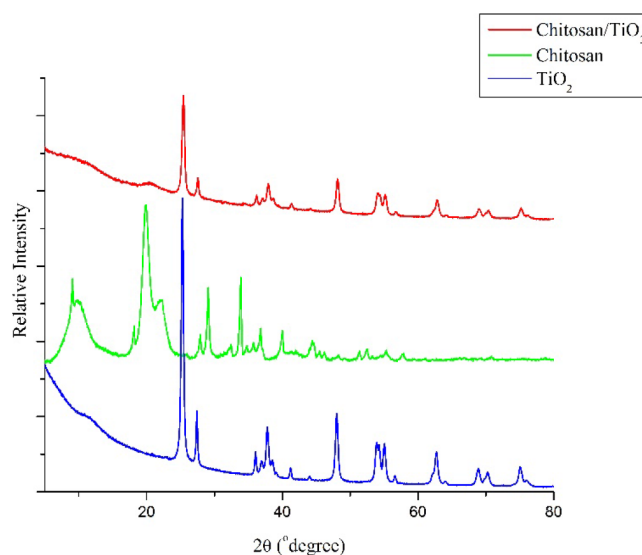
Fig. 3. XRD spectra of chitosan/TiO$_2$ composite.

shifted to a lower frequency, indicating chitosan deacetylation in acidic medium [23]. Accordingly, new –NH$_2$ groups were produced, but the peak intensity at 1570 cm^{-1} decreased in the composite because of chitosan bonding to TiO$_2$ through –NH$_2$.

3.4. TGA

The thermal behavior of chitosan/TiO$_2$ was analyzed by TGA, and results are shown in Fig. 5. For chitosan, 15% weight loss was observed at 40–145°C probably due to moisture evaporation. Remarkably, 145°C was higher than in free water (usually 110°C). The hydrogen bonding between a water molecule and chitosan was probably responsible for this high temperature. Decomposition then started at 200°C because of the degradation of acetylated and deacetylated units. In the case of chitosan/TiO$_2$, the decomposition temperature was prolonged with low weight loss.
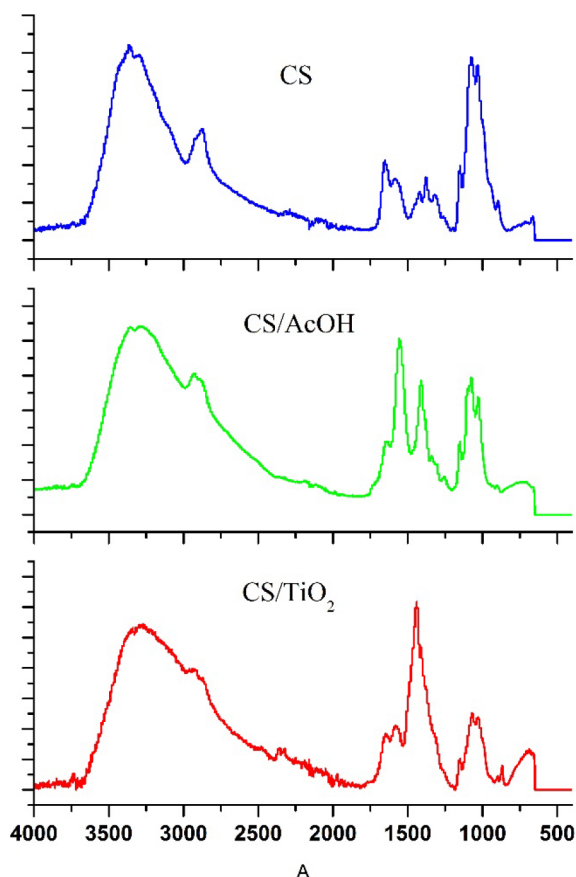
Fig. 4. FTIR spectra of chitosan/TiO₂ composite.

3.5. Weight-loss test

The weight-loss test was carried out in acidic medium. No weight loss was observed after 10 d. The chitosan dissolved in acidic medium because of the protonation of amino groups [28]. Thus, free amino groups were not retained in the chitosan/TiO₂ nanocomposite to be proton-

ated. As the composite was washed with NaOH, it may have helped induce hydrogen-bond formation between the amino groups of chitosan and TiO₂ by introducing a hydroxyl group into the matrix. The composite film was rigid and the shape was unaltered. The composite stability in acidic medium was an important finding because it indicated the potential industrial applications of chitosan/TiO₂ composite.
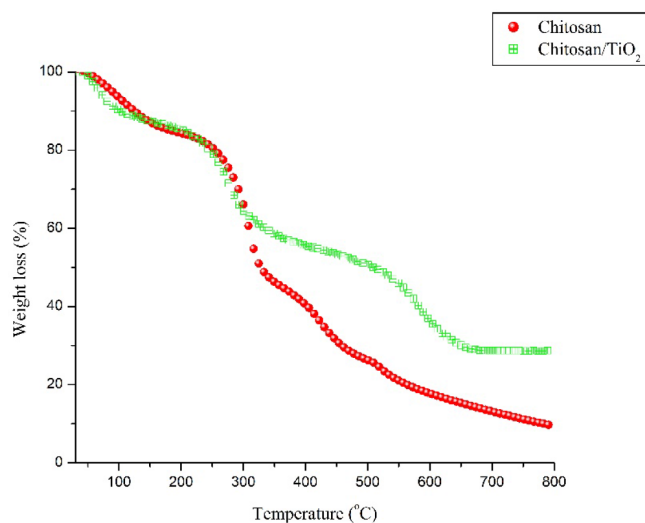
3.5.1. Key improvements compared with other literature findings

The main issue of chitosan is its instability in acidic medium. Although it has many important features, it cannot be applied industrially due to its chemical instability. The present experiment showed that chitosan/TiO₂ composite can have improved chemical stability of chitosan while maintaining the dye-adsorption capability.

3.6. Adsorption test

3.6.1. Adsorption isotherm

Adsorption data were analyzed by Langmuir isotherms and Freundlich adsorption models to determine the adsorption capacity of chitosan/TiO₂ nanocomposite. The adsorption mechanism can be predicted from the isotherm parameters.

The mathematical equation of the Langmuir isotherm [29] is as follows:

$$q_e = \frac{q_m k_a C_e}{1 + k_a C_e} \tag{3}$$

The linear form of Eq. (3) is as follows:

$$\frac{C_e}{q_e} = \frac{C_e}{q_m} + \frac{1}{k_a q_m} \tag{4}$$
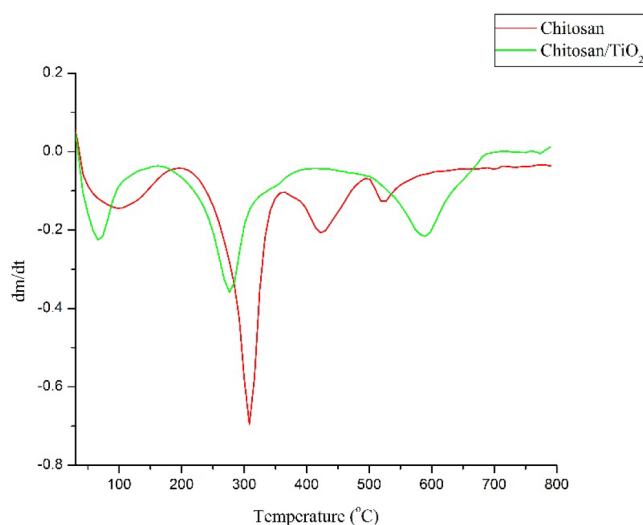
Fig. 5. (a) TGA and (b) DTG curves of chitosan/TiO₂ composite.
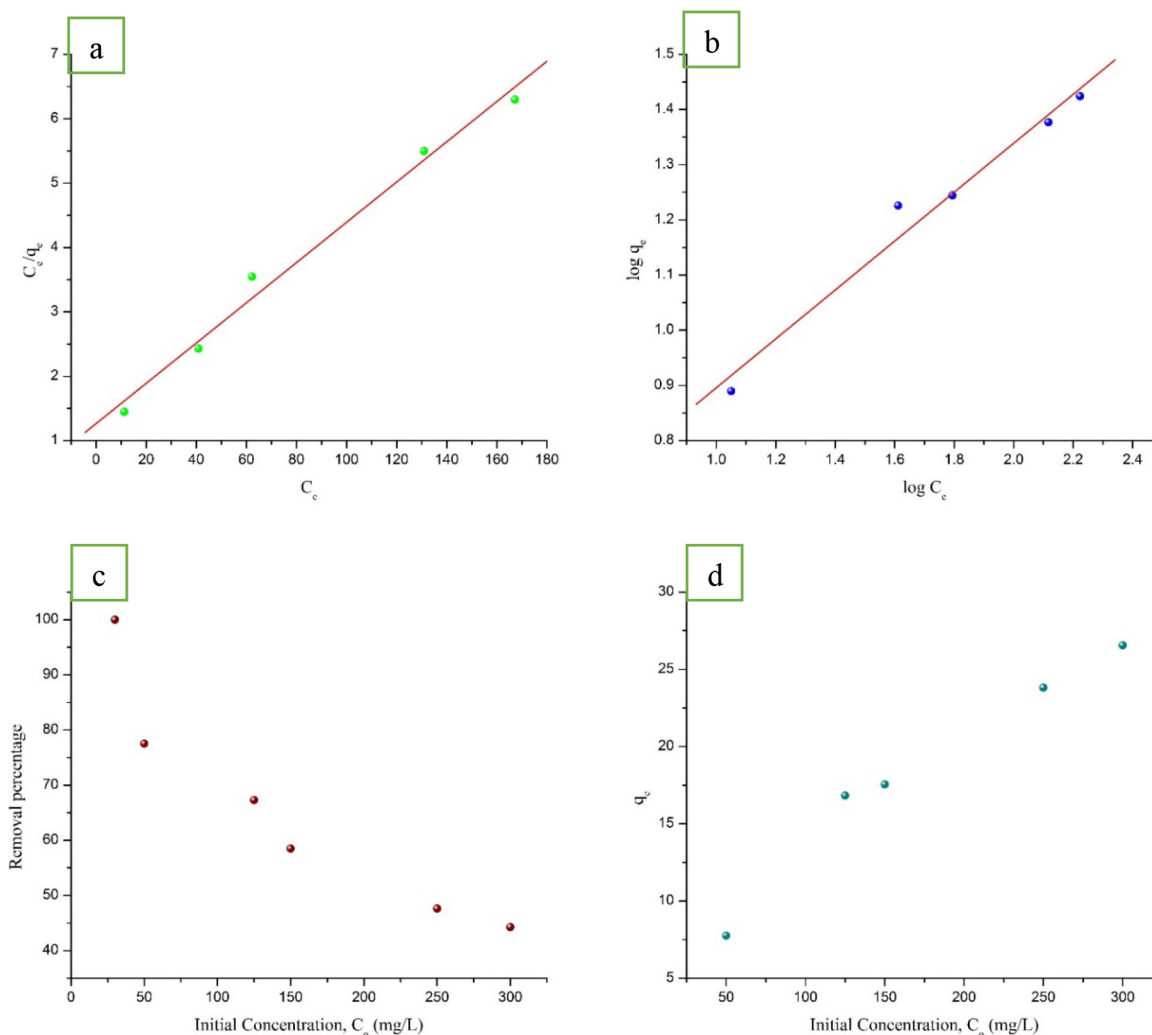
Fig. 6. (a) Langmuir isotherm, (b) Freundlich isotherm, (c) initial concentration vs. removal percentage, and (d) initial concentration vs. adsorption capacity.

where q_e (mg/g) is the Congo red adsorbed by chitosan/TiO$_2$ nanocomposite, C_e (mg/L) is the equilibrium concentration of Congo red, q_m is the adsorption capacity of the nanocomposite for Congo red, and K_a (L/mg) is a constant related to the affinity of the binding sites.

The favorability of the Langmuir isotherm can be evaluated by dimensionless adsorption intensity (R_L), which can be calculated as follows [30]:

$$R_L = \frac{1}{1 + K_a C_m} \tag{5}$$

where C_m is the maximum initial concentration of Congo red solution.

R_L represents the shape of the isotherm. The isotherm can be either unfavorable ($R_L > 1$), linear ($R_L = 1$), favorable

Table 1
Isotherm parameters

Adsorbate	Langmuir isotherm				Freundlich isotherm		
	q_m (mg/g)	K_a	R_L	R²	K_F	N	R²
Chitosan/TiO$_2$	32	0.02	0.14	0.99	2.8	2.25	0.98

Table 2
Comparison of adsorption capacities

Adsorbent	q_{max} (mg/g)	Reference
Chitosan hydrogel	318.47	[36]
Chitosan hydrogel beads impregnated with cetyl trimethyl ammonium bromide	162.3	[37]
Graphene oxide/chitosan fiber	294	[38]
Chitosan	320	[39]
TiO$_2$	112	[40]
Chitosan/TiO$_2$	32	Current study

$(0 < R_L < 1)$, or irreversible $(R_L = 0)$ depending on R_L. The calculated R_L was 0.14, which indicated that Congo red adsorption was favorable.

The Freundlich isotherm [31] can be used to identify the non-ideal adsorption of heterogeneous-surface-energy systems. It can be expressed by the following equation:

$$q_e = K_F C_e^{1/n} \qquad (6)$$

Usually, K_F indicates the adsorption capacity. The magnitude of $1/n$ signifies the favorability of the adsorption process.

Eq. (6) can be normalized using the logarithm to the following equation:

$$\log q_e = \log K_F + \frac{1}{n} \log C_e \qquad (7)$$

The $1/n$ values can define the order of isotherm. i.e., irreversible $(1/n = 0)$, favorable $(0 < 1/n < 1)$, and unfavorable $(1/n > 1)$ [15,32,33]. In this work, the value was 0.44, indicating favorable nature and heterogeneity of the adsorbents sites [16]. The experimental data of Congo red adsorption onto chitosan/TiO₂ nanocomposite well fitted both isotherm models. This finding suggested the mono layer adsorption of Congo red and the involvement of several functional groups [11,34]. The isotherm parameters are listed in Table 1. The adsorption capacity of the composite was 32 mg/g.

Table 2 shows that the adsorption capacity of chitosan/TiO₂ was lower than those previously observed for chitosan and TiO₂. The strong interaction between chitosan and TiO₂ may decrease the active sites for adsorption. Chitosan is also pH sensitive because of the protonation of amino groups in acidic medium [35]. The weight-loss test proved that the composite was sustained in an acidic medium, which indicated that free amino groups were not retained in the composite to be protonated. The adsorption capacity of chitosan largely depended on its amino groups, indicating that chitosan stability was achieved by sacrificing the adsorption capacity of chitosan and TiO₂.

3.6.2. Effect of initial concentration

Figs. 6c and 6d show the effects of the initial concentration of dye over adsorption capacity. The initial dye concentration was varied from 30 mg/L to 300 mg/L. The removal percentage of dye decreased with increased dye-solution concentration. This result may be attributed to the fact that the adsorption sites of the composite decreased at high concentrations of Congo red [29]. However, the value of adsorbed dye (q_e) increased with increased dye concentration. At high concentrations, the maximum collision occurred between the dye molecules and the active sites of the composite.

4. Conclusion

Chitosan/TiO₂ nanocomposite was synthesized and characterized by FESEM, FTIR, XRD, TGA, weight-loss test, and adsorption study. Results showed that the composite was stable in acidic medium. Strong bonding between chitosan and TiO₂ was observed by FTIR and XRD analyses. The adsorption isotherm followed the Langmuir and Freundlich models. The adsorption capacity of the composite was 32 mg/g. The removal percentage was higher when the initial concentration was low.

References

[1] V. Golob, A. Vinder, M. Simonič, Efficiency of the coagulation/flocculation method for the treatment of dye bath effluents, Dyes Pigm., 67 (2005) 93–97.

[2] S.S. Azhar, Dye removal from aqueous solution by using adsorption on treated sugarcane bagasse, Am. J. Appl. Sci., 2 (2005) 1499–1503.

[3] G. Annadurai, L.Y. Ling, J.-F. Lee, Adsorption of reactive dye from an aqueous solution by chitosan: isotherm, kinetic and thermodynamic analysis, J. Hazard. Mater., 152 (2008) 337–346.

[4] M. Tabatabaee, S.A. Mirrahimi, Photo degradation of dye pollutant on Ag/ZnO nanocatalyst under UV-irradiation, Orient J. Chem., 27 (2011) 65.

[5] Z. Zhang, Role of particle size in nanocrystalline TiO₂-based photo catalysts, J. Phys. Chem. B., 102 (1998) 10871–10878.

[6] S. Abbasizadeh, A.R. Keshtkar, M.A. Mousavian, Sorption of heavy metal ions from aqueous solution by a novel cast PVA/TiO₂ nanohybrid adsorbent functionalized with a mine groups, J. Ind. Eng. Chem., 20 (2014) 1656–1664.

[7] S. Abbasizadeh, A.R. Keshtkar, M.A. Mousavian, Preparation of a novel electro spun polyvinyl alcohol/titanium oxide nanofiber adsorbent modified with mercapto groups for uranium (VI) and thorium (IV) removal from aqueous solution, Chem. Eng. J., 220 (2013) 161–171.

[8] W. Cheung, Y. Szeto, G. McKay, Intra particle diffusion processes during acid dye adsorption onto chitosan, Bioresour. Technol., 98 (2007) 2897–2904.

[9] G.Z. Kyzas, Synthesis and adsorption application of succinyl-grafted chitosan for the simultaneous removal of zinc and cationic dye from binary hazardous mixtures, Chem. Eng. J., 259 (2015) 438–448.

[10] W.S. Wan Ngah, L.C. Teong, M.A.K.M. Hanafiah, Adsorption of dyes and heavy metal ions by chitosan composites: A review, Carbohyd. Polym., 83 (2011) 1446–1456.

[11] Y. Tao, Removal of Pb (II) from aqueous solution on chitosan/TiO₂ hybrid film, J. Hazard. Mater., 161 (2009) 718–722.

[12] A. Nithya, K. Jothivenkatachalam, Visible light assisted TiO₂-chitosan composite for removal of reactive dye, J. Environ. Nanotechnol., 3 (2014) 20–26.

[13] Z. Zainal, Characterization of TiO₂–Chitosan/Glass photo catalyst for the removal of a monoazo dye via photo degradation–adsorption process, J. Hazard. Mater., 164 (2009) 138–145.

[14] M.H. Farzana, S. Meenakshi, Synergistic effect of chitosan and titanium dioxide on the removal of toxic dyes by the photo degradation technique, Ind. Eng. Chem. Res., 53 (2013) 55–63.

[15] A. Özcan, Modification of bentonite with a cationic surfactant: an adsorption study of textile dye Reactive Blue 19, J. Hazard. Mater., 140 (2007) 173–179.

[16] Q. Baocheng, Adsorption behavior of Azo Dye CI Acid Red 14 in aqueous solution on surface soils, J. Environ. Sci., 20 (2008) 704–709.

[17] Z. Zakaria, Mechanical properties and morphological characterization of PLA/chitosan/epoxidized natural rubber composites, Adv. Mater. Sci. Eng., (2013).

[18] D. Jeevitha, K. Amarnath, Chitosan/PLA nanoparticles as a novel carrier for the delivery of anthraquinone: synthesis, characterization and in vitro cytotoxicity evaluation, Colloids Surf. B., 101 (2013) 126–134.

[19] N.E. Suyatma, Compatibilization method applied to the chitosan–acid poly (L-lactide) solution, J. Appl. Polym. Sci., 117 (2010) 3083–3091.

[20] C.-C. Tsai, H. Teng, Structural features of nanotubes synthesized from NaOH treatment on TiO_2 with different post-treatments, Chem. Mater., 18 (2006) 367–373.

[21] R. Zarate, Structural characterization of single crystals of sodium titanate nanowires prepared by hydrothermal process, J. Cryst. Growth, 310 (2008) 3630–3637.

[22] J. Ramírez-Salgado, E. Djurado, P. Fabry, Synthesis of sodium titanate composites by sol-gel method for use in gas potentiometric sensors, J. Eur. Ceram. Soc., 24 (2004) 2477–2483.

[23] J. Kumirska, Application of spectroscopic methods for structural analysis of chitin and chitosan, Mar. Drugs, 8 (2010) 1567–1636.

[24] R. Ramya, P. Sudha, J. Mahalakshmi, Preparation and characterization of chitosan binary blend, Int. J. Sci. Res. Publ., 2 (2012) 1–9.

[25] A. Çay, M. Miraftab, E.P.A. Kumbasar, Characterization and swelling performance of physically stabilized electro spun poly (vinyl alcohol)/chitosan nanofibres, Eur. Polym. J., 61 (2014) 253–262.

[26] A.M. Peiró, Low-temperature deposition of TiO_2 thin films with photo catalytic activity from colloidal anatase aqueous solutions, Chem. Mater., 13(8) (2001) 2567–2573.

[27] H. Homayoni, S.A.H. Ravandi, M. Valizadeh, Electro spinning of chitosan nanofibers: Processing optimization, Carbohydr. Polym., 77 (2009) 656–661.

[28] L. Yang, Swelling induced regeneration of TiO_2-impregnated chitosan adsorbents under visible light, Carbohydr. Polym., 140 (2016) 433–441.

[29] M. Kumar, R. Tamilarasan, V. Sivakumar, Adsorption of Victoria blue by carbon/Ba/alginate beads: Kinetics, thermodynamics and isotherm studies, Carbohydr. Polym., 98 (2013) 505–513.

[30] O. Ozdemir, Comparison of the adsorption characteristics of azo-reactive dyes on mezoporous minerals, Dyes Pigm., 62 (2004) 49–60.

[31] C.E. Zubieta, Reactive dyes remotion by porous TiO_2-chitosan materials, J. Hazard. Mater., 152 (2008) 765–777.

[32] M. Greluk, Z. Hubicki, Kinetics, isotherm and thermodynamic studies of Reactive Black 5 removal by acid acrylic resins, Chem. Eng. J., 162 (2010) 919–926.

[33] H. Yang, Q. Feng, Characterization of pore-expanded amino-functionalized mesoporous silicas directly synthesized with dimethyldecylamine and its application for decolorization of sulphonated azo dyes, J. Hazard. Mater., 180 (2010) 106–114.

[34] H. Zhang, Adsorption of iodide ions on a calcium alginate–silver chloride composite adsorbent, Colloids Surf. A Physicochem. Eng. Asp., 386 (2011) 166–171.

[35] L. Yang, Swelling induced regeneration of TiO_2-impregnated chitosan adsorbents under visible light, Carbohydr. Polym., 140 (2016) 433–441.

[36] S. Chatterjee, Congo red adsorption from aqueous solutions by using chitosan hydro gel beads impregnated with nonionic or anionic surfactant, Bioresour. Technol., 100 (2009) 3862–3868.

[37] S. Chatterjee, Enhanced adsorption of congo red from aqueous solutions by chitosan hydro gel beads impregnated with cetyl trimethyl ammonium bromide, Bioresour. Technol., 100 (2009) 2803–2809.

[38] Q. Du, Highly enhanced adsorption of congo red onto graphene oxide/chitosan fibers by wet-chemical etching off silica nanoparticles, Chem. Eng. J., 245 (2014) 99–106.

[39] A. Zúñiga-Zamora, J. Garcia-Mena, E. Cervantes-González, Removal of congo red from the aqueous phase by chitin and chitosan from waste shrimp, Desal. Water Treat., 57 (2016) 14674–14685.

[40] T. Şişmanoğlu, G. Pozan, Adsorption of congo red from aqueous solution using various TiO_2 nanoparticles, Desal. Water Treat., 57 (2016) 13318–13333.